

# Calibration of Multiple Landsat Sensors based on Pseudo-invariant Target Sites in Western Queensland, Australia.

Christina de Vries, Tim Danaher and Peter Scarth

Queensland Department of Natural Resources, Mines and Energy

80 Meiers Rd Indooroopilly QLD Australia 4068

christina.devries@nrm.qld.gov.au

**Abstract—** The Statewide Landcover and Trees Study (SLATS) has used both Landsat-5 TM and -7 ETM+ imagery to monitor short-term woody vegetation changes throughout Queensland. In order to analyse long-term vegetation change, time-based trends that are an artifact of the sensor system must be removed. Although the calibration trends of TM and ETM+ are well described, information on the calibration of the older Landsat-2 and -5 MSS sensors is relatively scarce. This paper describes the use of three pseudo-invariant target sites in western Queensland to achieve an operational calibration of TM and ETM+ data. Following the success of the current study, these targets will be used in the near future to achieve sensor specific calibrations for the Landsat-2 and -5 MSS SLATS data.

**Keywords-** Radiometric calibration; Landsat; pseudo-invariant targets

## I. INTRODUCTION

The Landsat series of satellites has been acquiring high-resolution global imagery continuously since the launch of the Landsat-1 satellite in 1972. The image data collected throughout the life of these satellites represent an important and unique source of information about the earth's surface, which is particularly useful for studying vegetation trends.

The Statewide Landcover and Trees Study (SLATS) [1] has used both Landsat-5 Thematic Mapper (TM) and -7 Enhanced Thematic Mapper Plus (ETM+) imagery to map tree cover and monitor the change in woody vegetation cover throughout Queensland (QLD), Australia since 1988. To date, SLATS monitoring has concentrated on change over relatively short time periods in image pairs, so any time-based trend in the calibration of the sensor has had little impact on the analysis. However, in order to analyse change over longer time periods any time-based trend, which is an artifact of the sensor system, must be removed. Additionally, if vegetation trends spanning multiple Landsat sensors are to be analyzed, a standardized approach to the calibration of each of the sensors involved (MSS, TM and ETM+) is required.

The launch of the Landsat-7 satellite in 1999, with the ETM+ sensor, provided access to data calibrated to better than 5% absolute [2]. Early in the Landsat-7 mission, the Landsat-5 and -7 satellites were placed in tandem orbit and the TM data were calibrated to the newer sensor to ensure calibration continuity between TM and ETM+ data [3]. Although the

calibration of the TM sensor at this cross-calibration date can be considered reliable, deterioration in the on-board calibration lamps has occurred over the life of the Landsat-5 satellite [4,5,6]. Consequently, a revised TM radiometric calibration procedure based on a lifetime radiometric calibration curve derived from the sensor's internal calibrator, cross-calibration with the ETM+ and vicarious measurements was adopted by the U.S. Geological Society (USGS) in May, 2003 [7].

Although the calibration trends of TM and ETM+ are well described, information on the calibration of the older Landsat-1, -2 and -5 MSS sensors is relatively scarce.

Landsat data utilized by SLATS consists of multiple date, complete coverages of the state of QLD (87 scenes) for the years 1988, 1991, 1995, 1997, 2003 (TM) and 1999 – 2003 (ETM+), as well as partial coverage for other years. SLATS also has Landsat-1, -2 and -5 MSS data ranging from 1972 to 1985. The majority of the TM and ETM+ imagery was purchased with Level 5 processing from the Australian Centre for Remote Sensing (ACRES). The TM Level 5 product is processed using the Canada Centre for Remote Sensing (CCRS) CAL2 calibration procedure outlined by [8,9]. In many cases the CCRS-CAL2 processing works well. However, inconsistencies in the gains of adjacent scenes from the same acquisition overpass have been identified for which no apparent reason can be ascertained.

The poor reliability of the CCRS-CAL2 calibration in even a few cases, along with the knowledge that the internal calibrator of Landsat-5 was not constant through time, led to the development of an operational SLATS calibration method independent of the CCRS-CAL2 processing. High-reflectance, pseudo-invariant target sites were chosen for a modified reflectance-based calibration approach. Previous work has used both dark and bright targets for radiometric normalization of multi-date images, with dark targets being used to characterize the atmosphere at each scene acquisition [10] and bright targets used to determine sensor responsivity (or gain) at the maximum reflectance value [2,11]. The main concern of this study is to determine the gain for both the TM and ETM+ sensors and thus bright targets have been used. Dark targets have not been used as in practicality, stable and effective dark targets are rare, particularly in areas where dark man-made features are scarce (such as western QLD). As such, the natural variation in the reflectivity of dark targets is likely to be larger than the atmospheric variation to be measured.

The advantage of using a reflectance-based technique is that it can supply an absolute radiometric calibration independent of the pre-flight and on-board calibrations [12]. Additionally, the chosen pseudo-invariant targets can be used to provide a comparable calibration for the MSS sensors for which there is a scarcity of calibration information.

In this work, the results of the SLATS calibration procedure for Landsat-5 TM and -7 ETM+, based on three pseudo-invariant target sites in western QLD, are presented.

## II. PSEUDO-INVARIANT TARGET SITE SELECTION

Pseudo-invariant targets were selected based on an analysis of surface reflectance and variability using a TM / ETM+ data archive of more than 350 images across Queensland. A minimum of four image dates per scene area were used in a preliminary analysis to select areas fulfilling two main criteria:

- high surface reflectance in bands 2, 4 and 5 (to select non-vegetated dry areas, to allow calibration of the sensor at a high response value and to increase the certainty of the calibration [4])
- low variance through time.

A detailed analysis using additional imagery (including MSS, TM and ETM+) for areas identified as potential calibration sites was then performed based on the above criteria and the following supplementary criteria [13]:

- high spectral uniformity across the site
- a near-lambertian surface to eliminate errors associated with bi-directional distribution factor effects
- located in western QLD to minimize atmospheric aerosol loading and decrease the probability of cloud
- located away from drainage areas
- accessible by 4WD vehicle.

Three sites were chosen which met the criteria outlined above. These sites are:

- “Warrabin” - located between Quilpie and Windorah in south-west QLD (26 17 00 °S, 143 39 15 °E). The area is a claypan surrounded by grassland and ironstone areas. Area = 44 375m<sup>2</sup>
- “Winton” - located south of Winton in central QLD (22 31 28 °S, 142 56 06 °E). The site is a claypan surrounded by shrubs and grassland. Area = 23 125m<sup>2</sup>
- “Dunrobin” - located on the Dunrobin property, north of Jericho in central QLD (22 40 25 °S, 146 08 04 °E). The site is a claypan. Area = 40 000m<sup>2</sup>

## III. METHODS

### A. Site surface reflectance measurements

Ground-based measurements were used to characterize surface reflectance at each of the three sites during 15 – 17 May 2003. Spectral measurements were collected along two 50m transects per site with an average of 10 samples taken per

transect. The Analytical Spectral Devices FieldSpec UV-VNIR CCD spectrometer and the Exotech 100C radiometer were used to sample the wavelengths corresponding to the those collected by the Landsat sensors. A level bubble alongside the fibre optic cable pistol grip was used to ensure vertical radiance measurements. Three irradiance measurements were taken at the beginning and ends of each transect using the cosine response corrected detector mounted on a leveled tripod. The site boundary and transect locations were recorded using differential global positioning system.

Post-field processing of the short-wave infrared (SWIR) irradiance measurements revealed that they were inaccurate, most likely due to equipment malfunction. To correct for this, the visible irradiance spectrum (from 400nm – 1000nm) was used, along with Total Ozone Mapping Spectrometer (TOMS) ozone (O<sub>3</sub>) climatology and precipitable water (PW) [14], to model the aerosol optical depth using MODTRAN software (v4.0). The modelled atmospheric variables were then used to predict the SWIR irradiance. The field radiance measurements were reliable and were ratioed to the predicted irradiance measurements to estimate reflectance in these wavelengths.

### B. Image processing

#### 1) Data

Thirty-five TM (ranging from 1987 to 2003) and twenty-one ETM+ (ranging from 1999 to 2003) scenes covering the three target sites were used. Earlier TM imagery was not available as archived TM imagery for Australia does not exist prior to mid-1986. Each scene was registered to an ETM+ geometric baseline image and a pixel resolution of 25m using a cubic convolution resampling method. Twelve additional TM scenes (from 1989 to 2004) with the same level of processing were used for assessing the accuracy of the TM calibration. The thermal band data was not included in the calibration.

#### 2) Obtaining image DN<sub>s</sub>

Each image was converted to the original digital number (DN) by removing the on-board calibration. The TM CCRS-CAL2 calibration was reversed by undoing the linear calibration applied by ACRES. The forward and reverse look-up-tables for each reference detector were combined in a least squares solution to determine the linear transformation used in the CCRS-CAL2 method.

The boundary coordinates were used to define the location of the site in each image. In some cases, the relative location of the site on the image was adjusted by one pixel to correct for image misregistration.

### C. Analysis of Gain

#### 1) Calculating gain

At-sensor radiance for each TM and ETM+ scene acquisition date was modelled from site reflectance using MODTRAN software (v4.0). TOMS O<sub>3</sub> climatology and meteorological observations of PW were used to estimate the atmospheric conditions for each image date. A constant visibility of 86km was used. This value represents the mean of seven aerosol optical depth observations at “Warrabin” from the MISR sensor, converted to visibility using the equation in [15].

The ratio of the mean image DNs to the at-sensor, MODTRAN-predicted radiance was used to calculate the gain for each Landsat spectral band, as in (1):

$$G_{\lambda} = (DN_{\lambda} - O_{\lambda}) / (L)_{\lambda} \quad (1)$$

where  $G_{\lambda}$  is the gain for the given band in counts per unit radiance (CPUR),  $DN_{\lambda}$  is the average DN for the site,  $O_{\lambda}$  is the mean scene offset in DN calculated on a scene by scene basis, and  $(L)_{\lambda}$  is the at-sensor, MODTRAN-predicted radiance.

The cross-calibration methodology described in [2] was used to calculate the responsivity coefficient ( $G_{i5}$ ) at “Warrabin” for the TM / ETM+ tandem image pair acquired on the 3<sup>rd</sup> June 1999. Modelled TOA reflectance was used to estimate the spectral band adjustment factor ( $B_i$ ).

## 2) Trend in gain through time

The determined gains were analyzed with GenStat 6.1 software using a linear regression with groups for any significant trends representing deterioration of the sensor through time. Published vicarious results [4] suggest that the TM calibration trend prior to 1987 is better represented by a non-linear trend. However, a linear relationship was considered suitable to describe the calibration trend for TM data in the SLATS archive (i.e. post-1987).

Data for each site were considered as a separate data group in the regression analysis to remove any significant between-site differences that were an artifact of errors in the site reflectance measurements. The “Winton” and “Dunrobin” data groups were normalized to the “Warrabin” data as the surface reflectance of the “Warrabin” site was characterized more thoroughly over two dates (as opposed to one date only at the other sites). Furthermore, a tandem image pair was available for the “Warrabin” data set allowing the calculation of a cross-calibration gain according to the methods in [2]. A sensitivity analysis was conducted to ensure that the groups adjustment did not significantly impact on the overall trend. The gain trends were forced through the cross-calibration gains from [2] at the tandem overpass date.

## D. Calibration check using independent data

A time-series of twelve TM images were used to assess the TM calibration derived above. The linear calibration equations from the Genstat analysis were used to calculate new time-dependent gains for each TM band. These gains were used to calculate radiance values from DNs at the “Warrabin” site for each new image date. TOA radiance values for each image date were also predicted from site reflectance (as described in C). The ratio of TOA image radiance to at-sensor, MODTRAN-predicted radiance was then calculated, as in (2):

$$R_{\lambda} = ((DN_{\lambda} - O_{\lambda}) / (A_{\lambda} * d + b_{\lambda})) / (L)_{\lambda} \quad (2)$$

where  $R_{\lambda}$  is the radiance ratio,  $A_{\lambda}$  and  $b_{\lambda}$  are the linear gain trend slope and offset, respectively and  $d$  is the image acquisition decimal date.

## IV. RESULTS

Although significant time-based trends (at  $p < 0.5$ ) are evident in all ETM+ bands, these trends represent a very minor

change in gain through time ( $< 0.1\%/year$  for bands 1 – 5,  $< 2\%/year$  for band 7). Overall, the gain results for ETM+ bands agree to within 5% of the pre-launch gain values. The results for each ETM+ band are presented in Fig. 1, along with error bars representing  $\pm 5\%$  of the pre-launch gain.

Significant time-based trends (at  $p < 0.5$ ) are evident in all TM bands, except band 3. These results compare closely to vicarious measurements published for TM. The fitted linear trends in gain for each TM band are presented in Fig. 2, along

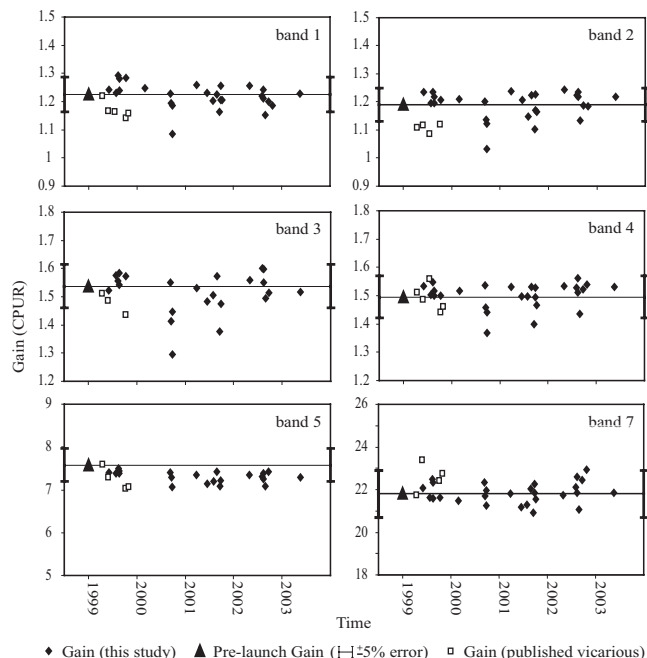


Figure 1. Landsat-7 ETM+ gains along with error bars representing  $\pm 5\%$  of the pre-launch gains and published vicarious gains from [11]. Note: trends for this study are not shown.

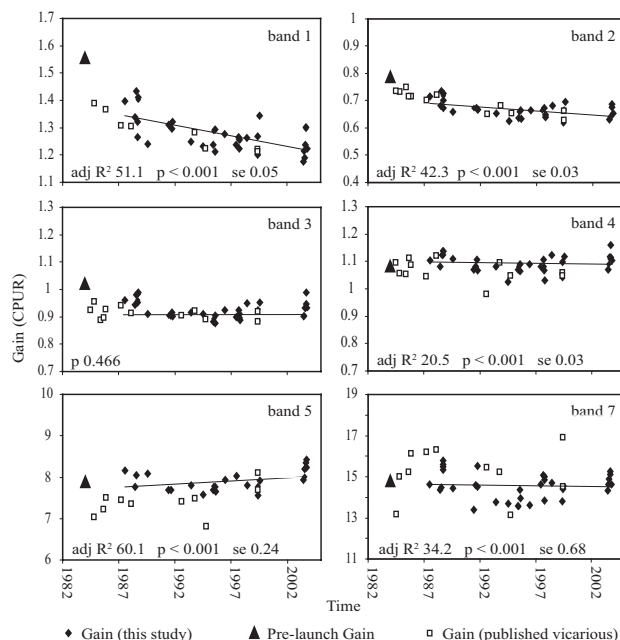


Figure 2. Trend in Landsat-5 TM gains through time, along with pre-launch and published vicarious gains from [4].

with the pre-launch gain and published vicarious measurements.

Absolute results in bands 5 and 7 for both sensors were not reliable due to spectrometer inaccuracies in the short-wave infrared spectrum. However, results for these bands are still presented in order to illustrate the relative gains.

Table 1 provides a comparison of  $G_{i5}$  for “Warrabin” to the cross-calibration results of [2]. These results fall within the  $\pm 3.5\%$  uncertainty level estimated for the tandem-based cross-calibration method for bands 2 – 7. The slighter higher band 1 results reflect the higher atmospheric uncertainty involved with the band 1  $B_i$  calculation.

No trends were identified in the radiance ratio in bands 1–4, and 7. However, a very small trend (both in significance  $p=0.042$  and slope) in band 5 was identified. These results indicate that the time-based calibration based on these pseudo-invariant target sites performs well operationally. Fine-tuning this technique in band 5 with more accurate atmospheric estimates and a larger number of TM data points may assist in refining the calibration trend. Fig. 3 illustrates the radiance ratio results for TM band 1 and 5.

TABLE I. TANDEM-BASED CROSS-CALIBRATION RESULTS FOR LANDSAT-5 TM ( $G_{i5}$  RESPONSIVITY COEFFICIENTS) COMPARED TO “WARRABIN” RESPONSIVITY COEFFICIENTS

Band	1999 cross-calibration ( $G_{i5}$ CPUR)	1999 “Warrabin” ( $G_{i5}$ CPUR)	Diff. relative to cross-calibration (%)
1	1.243	1.318	5.7
2	0.6561	0.68	3.49
3	0.905	0.936	3.35
4	1.082	1.11	2.52
5	7.944	7.999	0.69
7	14.52	14.903	2.57

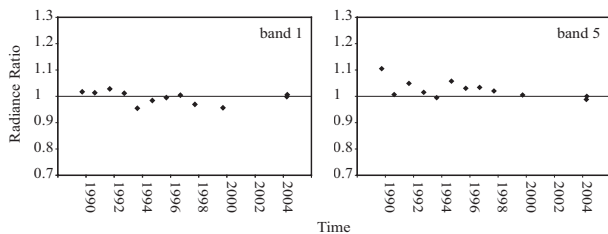


Figure 4. Radiance ratio for independent data at “Warrabin.”

## V. CONCLUSIONS AND FUTURE RESEARCH

The characterization and removal of time-based calibration trends in the SLATS TM data archive will eliminate the possibility of confusing calibration changes with long-term vegetation changes. Furthermore, the successful use of these targets in the calibration of TM and ETM+ indicates that these targets will be suitable for use in characterizing the calibration trends for other Landsat sensors.

The application of these calibration trends to the independent data (as illustrated in Fig. 3) highlights the success of the study for the operational requirements of SLATS. The radiance ratio for the independent data not only provides a

check of the calibration trend but also confirms that the final product used in the SLATS vegetation change studies is radiometrically normalized.

The time-based trends identified in this study are comparable to other vicarious measurements published to date, confirming the suitability of these sites as calibration targets. Furthermore, the responsivity coefficients derived for “Warrabin” from tandem data agree to within  $\pm 2\%$  of the cross-calibration gains obtained in [2] in bands 2 – 7, and within 4% in band 1.

Following the success of the current study, these pseudo-invariant targets will be used in the future to achieve sensor specific calibrations for the MSS data required by SLATS.

## ACKNOWLEDGMENTS

The authors thank C. Smith, ACRES for provision of tandem-image data and for sharing his expertise in ACRES data processing. We also thank S. Phinn, Biophysical Remote Sensing Group, University of Queensland for the use of the spectro-radiometers.

## REFERENCES

- [1] SLATS, “Statewide Landcover and Trees Study,” <http://www.nrme.qld.gov.au/slats/index.html>, 2004.
- [2] NASA, “Landsat 7 Science data users handbook,” [http://ftpwww.gsfc.nasa.gov/IAS/handbook/handbook\\_toc.html](http://ftpwww.gsfc.nasa.gov/IAS/handbook/handbook_toc.html), 2004.
- [3] P. Teillet, *et al.*, “Radiometric cross-calibration of the Landsat-7 ETM+ and Landsat-5 TM sensors based on tandem data sets,” *Rem. Sens. Env.*, vol.78, pp.39-54, 2001.
- [4] K. Thome, B. Markham, J. Barker, P. Slater, and S. Biggar, “Radiometric calibration of Landsat,” *Photogramm. Eng. Rem. Sens.*, vol.63, pp.853-858, 1997.
- [5] D. Helder, W. Bonyck, and R. Morfitt, “Absolute calibration of the Landsat thematic mapper using the internal calibrator,” *Proc. 1998 IGARSS*, Seattle, Washington, pp.2716-2718, 1998.
- [6] B. Markham, J. Seiferth, J. Smid, and J. Barker, “Lifetime responsivity behavior of the Landsat-5 Thematic Mapper,” *Proc. SPIE Conf. 3427*, San Diego, California, pp.420-431, 1998.
- [7] G. Chander, and B. Markham, “Revised Landsat-5 TM radiometric calibration procedures and post-calibration dynamic ranges,” *IEEE Trans. Geosc. Rem. Sens.*, vol.41, pp.2674-2677, 2003.
- [8] D. Helder, “Final report for Landsat TM and MSS data relative radiometric calibration study,” USGS, EROS Data Centre, Dakota, 1992.
- [9] ACRES, “ACRES (CCRS) Landsat thematic mapper digital data format description,” <http://www.ga.gov.au/acres/techdocs/techdoc.htm>, 1999.
- [10] J. Hill, “Radiometric correction of multi-temporal thematic mapper data for use in agricultural land-cover classification and vegetation monitoring,” *Rem. Sens. Env.*, vol.12, pp.1471-1491, 1991.
- [11] K. Thome, “Absolute radiometric calibration of Landsat 7 ETM+ using the reflectance-based method,” *Rem. Sens. Env.*, vol.78, pp.27-38, 2001.
- [12] K. Thome, “Ground-look radiometric calibration approaches for remote sensing imagers in the solar reflective,” *ISPRS Commission 1*, Denver, Colorado, 10-15 Nov 2002.
- [13] K. Scott, K. Thome and M. Brownlee, “Evaluation of the Railroad Valley Playa for use in vicarious calibration,” *Proc. SPIE Conf. 2818*, pp.158-166, 1996.
- [14] S. Jeffrey, J. Carter, K. Moodie, and A. Beswick, “Using spatial interpolation to construct a comprehensive archive of Australian climate data,” *Env. Modelling and Software*, vol.16/4, pp.309-330, 2001.
- [15] E. Vermote, D. Tanré, J. Deuzé, M. Herman, and J. Morcrette, “6S User Guide Version 2,” 1997.